G&G
Gem News International

Contributing Editors
Emmanuel Fritsch, *University of Nantes, CNRS, Team 6502, Institut des Matériaux Jean Rouxel (IMN), Nantes, France* (fritsch@cnrs imn.fr)
Gagan Choudhary *Gem Testing Laboratory, Jaipur, India* (gagan@gjepcindia.com)
Christopher M. Breeding, *GIA, Carlsbad* (christopher.breeding@gia.edu)

COLORED STONES AND ORGANIC MATERIALS

Large star emerald. Star emeralds are rare specimens, and most are found in either Brazil or Madagascar. In 1999, Manuel Marcial de Gomar (Key West, Florida) purchased a 1,000-carat parcel of rough emeralds from Diallo Mahmoud, an independent emerald dealer based in Africa. Mahmoud noted that the parcel came from Madagascar. Marcial de Gomar later noticed that some crystals showed indications of chatoyancy. He chose this particular piece thinking it could be cut to produce a cat's-eye emerald. Miami-based cutter Jone Ribeiro cut the stone into a 25.86 ct double cabochon (figure 1). Marcial de Gomar put the stone into his personal collection, where it stayed for 13 years, until independent gemologist and appraiser Martin Fuller examined Marcial de Gomar's collection in 2013. Both experts recognized that this emerald was a star and not a cat's eye. It was subsequently sent to GIA's Carlsbad laboratory for an identification report.

The stone is described as an oval double cabochon natural star emerald. The asterism was caused by minute hexagonal fluid inclusions oriented parallel to the basal plane of the crystal (e.g., Spring 2004 GNI, p. 104; K. Schmetzer, et al., "Asterism in beryl, aquamarine, and emerald—an update," *Journal of Gemmology*, Vol. 29, No. 2, 2004, pp. 66–71). They exhibit thin film interference with direct, pinpointed light that caused the asterism, as well as rainbow colors seen at high magnification (figure 2). Prior to this report, very few asteriated emeralds were recorded (e.g. Fall 1995 GNI, p. 206; Spring 1995 GNI, pp.

Figure 1. A weak, six-rayed star is visible in this 25.86 ct emerald cabochon. Photo by Robert Weldon/GIA, courtesy of Manuel Marcial de Gomar.

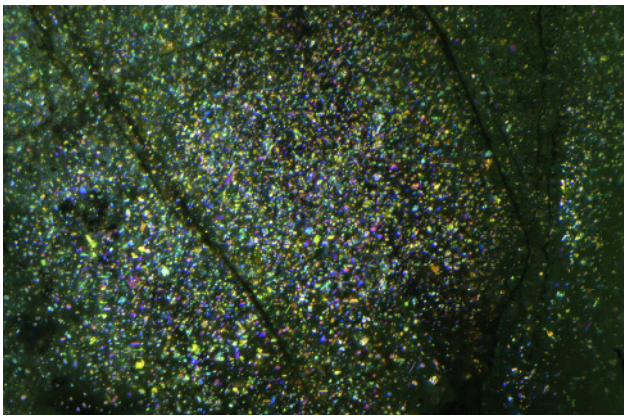

Figure 2. Minute fluid inclusions oriented parallel to the basal plane of the crystal are the cause of this emerald's asterism. The inclusions exhibit thin-film interference, causing rainbow colors that are visible at high magnification. Photo by Nathan Renfro; field of view 1.8 mm. Courtesy of Manuel Marcial de Gomar.

Editors' note: Interested contributors should send information and illustrations to Stuart Overlin at soverlin@gia.edu or GIA, The Robert Mouawad Campus, 5345 Armada Drive, Carlsbad, CA 92008.

Gems & Gemology, Vol. 51, No. 3, pp. 334–345.

Figure 3. The 4.40 ct natural red rutile on the left was compared with a 4.47 ct orange flame-fusion synthetic rutile. Photo by C.D. Mengason.

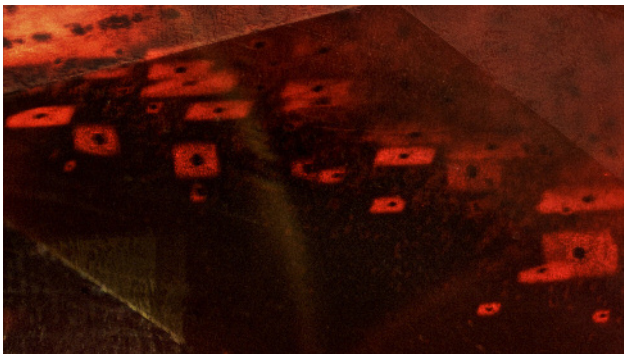

Figure 5. Near the girdle, rectangular tabular inclusions are observed under fiber-optic illumination. Photomicrograph by Ziyin Sun; field of view 2.43 mm.

60–61; Spring 2002 GNI, p. 104; Summer 2006 GNI, pp. 171–172). This is the eleventh, and largest, star emerald known to date.

Carl Chilstrom
GIA, Carlsbad

Natural faceted red rutile. The Carlsbad laboratory recently received a 4.40 ct dark red marquise brilliant (figure 3, left) for examination. Standard gemological testing revealed a refractive index that was over the limit of the RI liquid, as well as a hydrostatic specific gravity (SG) of 4.27. The specimen was inert to both long-wave (LW) and short-wave (SW) UV. Under reflected light, it showed a metallic luster. Raman testing identified the material as rutile. To distinguish it as natural or synthetic rutile, we compared it with a known flame-fusion orange synthetic rutile sample (figure 3, right).

Under magnification, the most distinctive internal characteristic of the dark red specimen was an octagonal blockage with a long growth tube extending to the surface (figure 4). Near the girdle, some unknown rectangular tabular inclusions were also observed, which were not identified by Raman spectroscopy (figure 5). Both internal features indicated the specimen was natural rutile. Straight and angular growth banding was also observed (figure 6). Raman spectroscopy for both the red sample and the orange synthetic revealed major peaks at 610, 446, and 242 cm^{-1} and minor peaks at 818, 707, and 319 cm^{-1}, confirming their identity as rutile (see the RRUFF database at rruff.info).

Laser ablation–inductively coupled plasma–mass spectrometry (LA-ICP-MS) revealed that the dark red rutile had a composition of 98.2% TiO_2 and 1.5% Fe_2O_3 by weight, with traces of Mg, Al, Si, Ca, Sc, V, Cr, Cu, Zn, Zr, Nb, Cd, In, Sn, Sb, Hf, Ta, W, Pb, and U. The presence of Nb (176.81–296.93 ppmw), Ta (15.13–25.81 ppmw), Hf (0.15–0.40 ppmw), Zr (3.29–4.84 ppmw), Pb (0.01–0.56 ppmw), and U (0.07–0.27 ppmw) suggested a natural origin. The orange synthetic rutile contained 99.9% TiO_2, plus traces of Mg, Si, Cr, Co, Cu, and Zn. Traces of iron (1.66 ppmw, 0.0238% Fe_2O_3 by weight) were also detected. Synthetic

Figure 4. In this natural red rutile, an octagonal blockage is capped at the end of the growth tube. Photomicrograph by Ziyin Sun; field of view 1.40 mm.

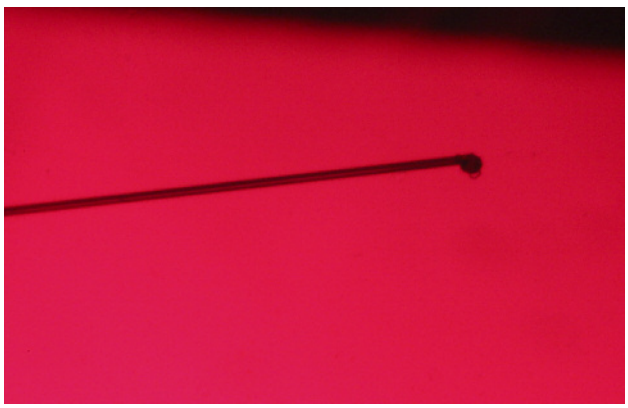

Figure 6. The natural rutile shows straight and angular growth banding. Photomicrograph by Ziyin Sun; field of view 4.92 mm.

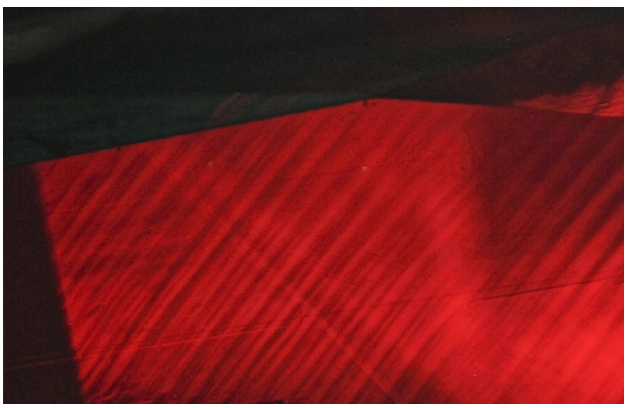

Figure 7. Face-up view of two quartz cabochons from Brazil, weighing 116.95 ct (left) and 44.12 ct (right) with cross-like quartz inclusions. Photo by Jaroslav Hyršl.

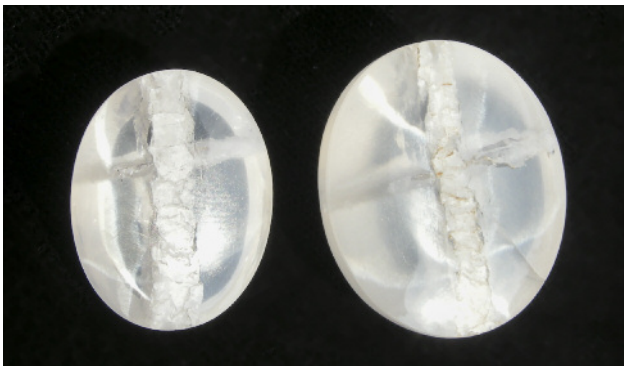

Figure 8. The stars in the quartz samples, seen from the base, are eye-visible in sunlight. Photo by Jaroslav Hyršl.

rutile boules created by the Verneuil process have an orange color with 0.04% Fe_2O_3 and a clear reddish color with 0.2% Fe_2O_3 (C.H. Moore, Jr. and R. Dahlstrom, "Synthetic rutile crystal and method for making same," U.S. Patent 2792287). The red specimen's lower chemical purity indicates natural origin.

Visible spectra of both stones were taken. The red bodycolor of the natural rutile matched the transmission window between 650 and 700 nm in the red portion of the spectrum, which was likely caused by iron.

Although rutile is a common inclusion in many minerals, the few crystals that are faceted usually weigh less than 1 ct. This faceted stone was very rare because of its large size. It was the first faceted natural rutile examined by GIA's Carlsbad laboratory.

Ziyin Sun (zsun@gia.edu), Amy Cooper, and Adam Steenbock
GIA, Carlsbad

Rare "star and cross" quartz from Brazil. The author purchased two very unusual quartz samples (figure 7) in Brazil in 2015. Both were cut as cabochons with a slightly curved bottom; one weighed 116.95 ct (35.0 × 30.3 × 15.6 mm), while the other weighed 44.12 ct (28.3 × 22.3 × 10.0 mm). The larger cabochon was slightly milky, while the smaller one was almost clear. Both showed a strong six-rayed star when illuminated (figure 8). The stars were centered on the top of the cabochons, which indicates that both were cut perpendicular to the c-axis. The most unusual feature was a cross-like inclusion in both stones. It was white and coarse-grained, only slightly translucent. The longer part of both crosses measured about 4 mm wide. The shorter part had a thickness 1.5 to 2 mm and the angle of the intersection was about 85 degrees in both cabochons, which meant that the two specimens were probably cut from the same crystal. RI results and Raman analysis showed the cross to be quartz, rather than a foreign mineral. The origin of the cross inclusions is uncertain, but they are strong evidence of nature's ability to produce rarities.

Jaroslav Hyršl (hyrsl@hotmail.com)
Prague

Serpentine cabochon with unusual olive green color. Serpentine is a common ornamental stone in the jewelry trade. With colors ranging from yellowish green to deep green, it is commonly used as an imitation of jadeite or nephrite.

Recently, the Gem Testing Laboratory at the Shijiazhuang University of Economics in Hebei, China, examined an olive green cabochon (figure 9) weighing 4.05 ct and measuring approximately 12 × 8 × 6 mm, reportedly purchased from China's Shandong province. The sample was relatively clean, with a vitreous luster and without any eye-visible inclusions. Without magnification, it resembled high-quality jadeite jade. Standard gemological testing gave

Figure 9. This 4.05 ct translucent serpentine is unusual for its olive green color and lack of impurities. Photo by Yanjun Song.

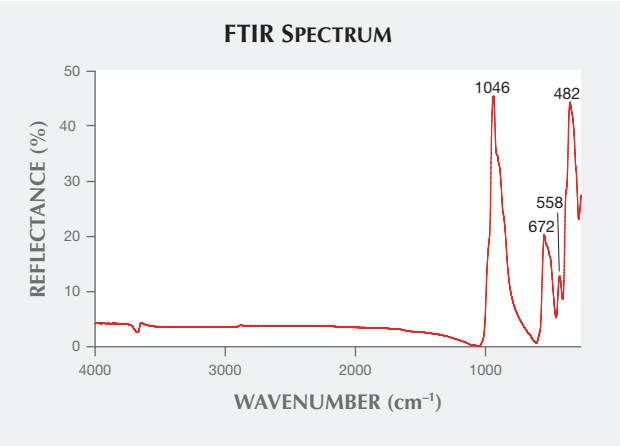

Figure 10. The FTIR spectrum of the 4.05 ct emerald-green cabochon sample exhibits characteristic peaks at 1046, 672 and 482 cm^{-1}, all consistent with serpentine.

a spot RI of 1.56 and a hydrostatic SG of approximately 2.56; the sample was inert to both LW and SWUV. These properties are consistent with serpentine. Four main peaks were observed in the 1100–400 cm^{-1} region of the infrared reflectance spectrum (figure 10). The two peaks at about 1046 and 482 cm^{-1} were related to the fundamental Si-O vibrations. The remaining two peaks at 672 and 558 cm^{-1} are attributed to the OH^- and Mg-O vibrations, respectively, confirming the sample's identity as antigorite, a species in the serpentine family.

EDXRF was used to differentiate the sample from the common "Xiuyu" variety of serpentine, from China's Liaoning province. Testing revealed that both Cr and Ni were significantly higher in this material than in serpentine from Liaoning, indicating that the specimen may have formed from the serpentinization of mafic-ultramafic rocks. We suspect it may have originated in Taian City in Shandong province, which is famous for "Taishan jade," a newfound variety of serpentine.

Although serpentine is common in the Chinese market, this was the first time our researchers have encountered a sample of such high quality.

Yanjun Song and Lu Zhang
Shijiazhuang University of Economics, Hebei, China

Thai-Myanmar petrified woods. Petrified woods (figure 11, left) have long been used as a gem and ornamental material due to their beauty, luster, durability, and relative rarity. Certain minerals (mainly quartz, opal, or moganite) crystallize or precipitate in the hollow cavities and cells of the woods in a fossilization process. Fossil trading is government regulated in some countries, and gemologists should know the useful identifying characteristics of petrified woods, which can be misidentified as jasper and agate. With this in mind, the author examined Thai-Myanmar petrified wood samples, fashioned as cabochons (figure 11, right), for gemological characterization.

More than 100 Thai samples were collected from the four localities shown in figure 12: Tak, in Ban Tak-Oke (TAK); Khon Kaen, in Ban Hin Khao (BHK); Chaiyaphum, in Noen Sa Nga (CYP); and Nakhonratchasima, in Kroke Duan Ha (KDH). About 100 Burmese samples were donated by carvers from Mae Sai in Chiang Rai province (MYR), near the border of Thailand and Myanmar. Thai specimens were collected from either Quaternary gravel beds of fluvial deposits or the high-terrace sands and grav-

Figure 11. Left: Petrified woods are carved and sold as ornamental gem materials, such as these specimens from the Mae Sai market near the Thai-Myanmar border. Right: A few of the cabochons from this study. Photos by Seriwat Saminpanya.

Figure 12. A map showing the localities in Thailand and Myanmar where the petrified wood samples originated. Adapted from Saminpanya and Sutherland, 2013.

els of paleorivers. Tektite grains found in the sediments date back 700,000 to 900,000 years (P. W. Haines et al., "Flood deposits penecontemporaneous with ~0.8 Ma tektite fall in NE Thailand: Impact-induced environmental effects?" *Earth and Planetary Science Letters*, Vol. 225, 2004, pp. 19–28).

Thirty-eight samples (all but seven from Thailand) were tested by standard gemological methods, Raman spectroscopy, and X-ray diffraction (XRD). Thirty-seven of these came from dicotyledonous plants, indicated by vascular bundles concentrated in an outer ring of active growth. Periods of slow (winter) and fast (summer) growth create the growth rings in the trunk. One sample came from a palm tree, and had vascular bundles dispersed throughout the trunk.

The rough surfaces may have been altered and stained by soil or iron oxides, resulting in black, brown, cream, white, and red coloration. Colorless areas and different shades of brown, black, gray, white, cream, yellow, orange, and red appeared below the surface. Some samples exhibited color banding. Most Thai samples were opaque or nearly opaque; those from Myanmar were translucent and lighter in tone. The surfaces showed varying degrees of luster and fracturing. RI ranged from 1.425 to 1.543 (tested at the flat polished base of the cabochon), and SG ranged from 1.963 to 2.616. Most samples fluoresced weak to moderate chalky white under LWUV, but some were inert or showed very weak white fluorescence.

A gemological microscope can often reveal a well-preserved wood grain structure in petrified wood samples.

Studies of wood structure generally involve the transverse, tangential, and radial sections of the trunk (R.F. Evert, *Esau's Plant Anatomy: Meristems, Cells, and Tissues of the Plant Body: Their Structure, Function, and Development*, 3rd ed., John Wiley & Sons, Hoboken, New Jersey, 2006, pp. 203, 292–296). A transverse section of one of the samples (figure 13) showed several tiny oval-shaped pores filled with quartz or opal (e.g., S. Saminpanya and F.L. Sutherland, "Silica phase-transformations during diagenesis within petrified woods found in fluvial deposits from Thailand-Myanmar," *Sedimentary Geology*, Vol. 290, 2013, pp. 15–26). The samples also showed thin parallel rays, groups of cells oriented perpendicular to the trunk's main axis. In some samples, the parenchyma (the most common plant tissue cells) consisted of pale lines or bands running across the rays. Others showed parenchyma surrounding a pore on the long and parallel wood grains of the tangential section, or dark-colored pores extending the length of the trunk. On the radial section, the pores ran the length of the trunk, with wood grains perpendicular to the pores.

Raman spectra were characteristic of opal (according to the RRUFF database, rruff.info), quartz, and moganite (K.J. Kingma and R.J. Hemley, "Raman spectroscopic study of microcrystalline silica," *American Mineralogist*, Vol. 79, 1994, pp. 269–273). Figure 14 shows the peaks for the TAK, BHK, and CYP samples; peaks for KDH (which included opal) and MYR samples were previously presented (Saminpanya and Sutherland, 2013). Most of the quartz material displayed peaks at 354, 395–397, and 464–466 cm^{-1}, with different colors within a sample exhibiting different peak intensities. Some samples showed only major peaks of quartz at 464–466 cm^{-1}. Moganite was mixed with quartz in one sample apiece from CYP, KDH, and MYR, indicated by peaks at 503–506 cm^{-1}, close to the reference peak of 501 cm^{-1} (Kingma and Hemley, 1994). Two KDH samples showed bands centered at 1587 and 1607 cm^{-1}, characteristic of opal (Saminpanya and Sutherland, 2013), which was probably responsible for the weak to moderate chalky white fluorescence in some of the samples.

XRD showed that the quartz peaks had an average 2Θ of 21.0, 26.7, 36.6, 39.6, 40.4, 42.5, 45.9, 50.2, and 55.0 degrees; the opal-CT peaks had an average 2Θ of 20.7, 21.7, 36.0, 44.0, and 56.9 degrees (again, see rruff.info). Quartz appeared in the XRD peaks of samples from all localities, but the opal-CT was found only in samples from KDH and MYR. The diffractogram of opal-CT in one sample from KDH appeared noisy. This may be due to its amorphous nature, though extending the XRD scan times may improve the resolution of the peaks. At this stage, XRD can only detect quartz and opal from these samples.

Figure 13. Oval pores and rays (wavy white lines) are seen on a transverse section of this petrified wood sample, and the growth rings are visible as two lines crossing the image. Photomicrograph by Seriwat Saminpanya; field of view 10 mm.

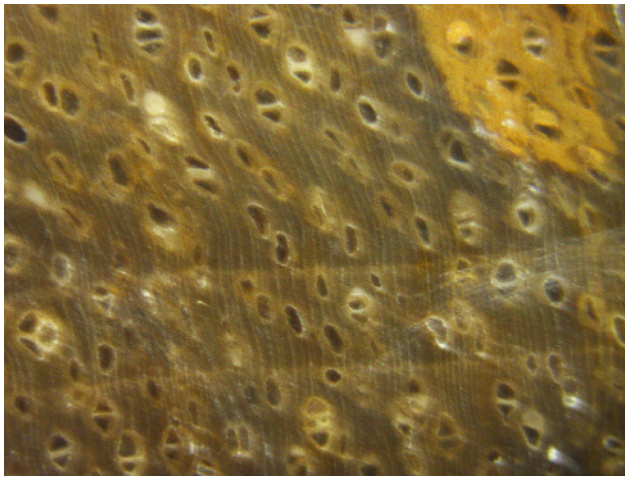

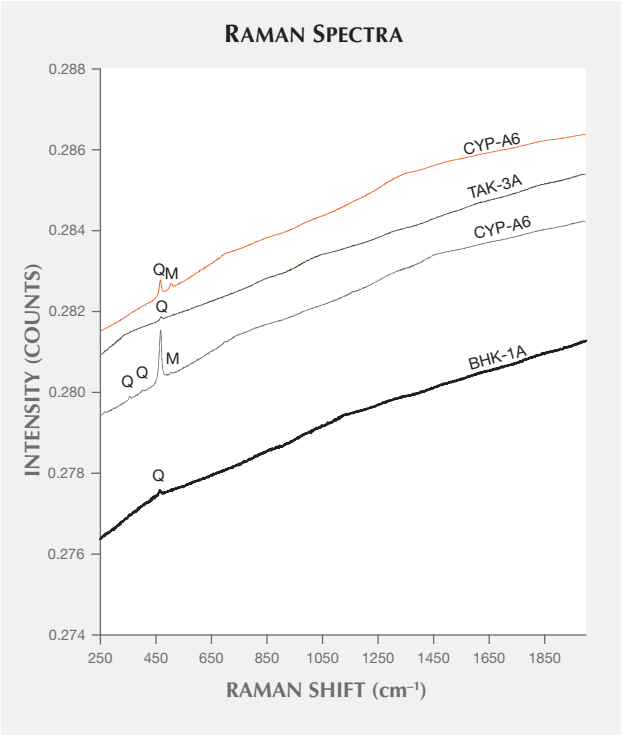

Figure 14. Raman spectra of petrified wood samples from Chyaphum (CYP), Tak (TAK), and Khon Kaen (BHK) with quartz (Q) peaks at 465 cm^{-1}. Samples from Chyaphum show a moganite (M) peak at 503–506 cm^{-1}.

Seriwat Saminpanya
Srinakharinwirot University, Bangkok

SYNTHETICS AND SIMULANTS

Coated rock crystal imitation of ruby. Recently the Dubai Central Laboratory received for identification a rough stone

Figure 15. This coated rock crystal imitation of ruby has a brown skin. Photo by Nazar Ahmed Ambalathveettil, Dubai Central Laboratory.

Figure 16. The rock crystal shows dark red under transmitted light to imitate ruby. Photo by Nazar Ahmed Ambalathveettil, Dubai Central Laboratory.

weighing 616.93 g and measuring approximately 114.3 × 65.8 × 53.0 mm (figure 15). Most of it was covered by a brown skin, while other parts were transparent. Viewed through one of the transparent areas, the stone showed a red color. Under oblique light, the stone appeared dark red, with some areas that were colorless (figure 16).

Microscopic examination with transmitted light revealed negative crystals, fingerprints, and two-phase inclusions. Observation of the transparent and opaque areas on the surface showed red, green, and blue areas of coating that could be removed using sharp needles. These coated areas gave the stone a purplish red color overall, but some transparent areas appeared colorless under transmitted light and no coating was observed there. The stone's SG was 2.60. The coated area gave a patchy chalky blue and purple reaction under LWUV and was inert to SWUV. Specific gravity and inclusions indicated a rock crystal; this was confirmed by Raman spectroscopy.

This was the first time the Dubai Central Laboratory had identified such a large coated rough stone imitating ruby.

Nazar Ahmed Ambalathveettil (nanezar@dm.gov.ae) and Mohamed Karam
Gemstone Unit, Dubai Central Laboratory
Dubai, United Arab Emirates

Color-change synthetic cubic zirconia as peridot imitation. Peridot is a common gemstone in the jewelry industry; however, it is rarely simulated using substances other than glass (Summer 2004 Lab Notes, p. 165). The State Gemological Centre of Ukraine recently received for identification an

Figure 17. This synthetic cubic zirconia imitation of peridot, with an estimated weight of 4.50 ct, is shown in daylight (left) and incandescent light (right). Photos by Igor Iemelianov; field of view 13.20 mm.

oval-cut gemstone, with an estimated weight of 4.50 ct, set in a ring. The stone was greenish yellow in daylight (figure 17, left) and orangy yellow in incandescent light (figure 17, right). The client who submitted the ring specifically wished to know if the center stone was peridot. The sample was transparent and isotropic, with an RI of 2.150 (measured by a refractive index meter) and was inert to both SW and LWUV radiation. Microscopic examination revealed no inclusions. The measured relative reflectivity (RR 65–67), obtained using a Presidium DuoTester, clearly matched that of cubic zirconia, a result in line with the other gemological observations. This allowed us to identify the stone as cubic zirconia. Chemical analysis with EDXRF showed Zr and Y, with minor Pr and Nd. These impurities can cause color change in this stone. Using fiber-optic light with the spectroscope, we observed a complex set of absorption lines in both the orange and green-blue regions (the same measurement can be seen at http://www.gemlab.co.uk/peridot.html). This study shows the importance of studying a variety of simulants, even those for less-expensive gems such as peridot.

Iurii Gaievskyi (gaevsky@hotmail.com)
and Igor Iemelianov
State Gemological Centre of Ukraine, Kiev

Coral inclusions in plastic. Composites assembled from opaque-to-translucent and transparent gem materials such as turquoise, chalcedony, opal, chrysocolla, tourmaline, and peridot have become popular over the past few years, as evidenced by the number of samples received for identification at the Gem Testing Laboratory in Jaipur, India. Recently, we examined an orangy red bead of plastic (figure 18) with embedded fragments of coral.

The round bead weighed 37.50 ct and measured 20.62 × 20.57 × 14.02 mm. The bead was represented as coral, but its smooth texture along with the luster was sufficient enough to rule out that possibility. A few spots of lighter color (again, see figure 18), visible to the unaided eye, made it more interesting. Under strong fiber-optic light, minute transparency was observed, while microscopic examination revealed numerous gas bubbles scattered throughout the bead. Sharp boundaries between the lighter spots and the host bead suggested that these spots of lighter color were actually fragments of some other material. These randomly oriented fragments also displayed some concentric radiating structures (figure 19, left), typically seen in carbonate-type corals. Some chips also showed elongated sections (figure 19, right), along with some whitish to faintly colored areas.

Although the bead was obviously an artificial product, its major component was still to be identified. A spot RI of

Figure 18. This 37.50 ct plastic bead contained visible fragments of carbonate-type coral (the lighter spots). Photo by Gagan Choudhary.

Figure 19. Some of the fragments embedded in the plastic bead displayed concentric radiating structures (left), typically seen in carbonate-type coral, while others show elongated sections (right). Also note the sharp edges and whitish to faintly colored areas of the fragments. Photomicrographs by Gagan Choudhary; field of view 5.08 mm.

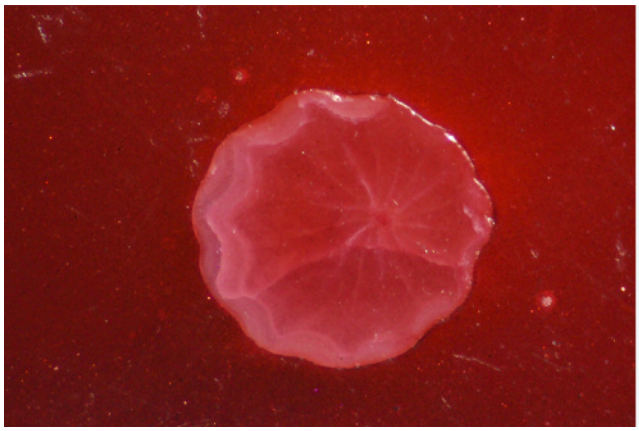

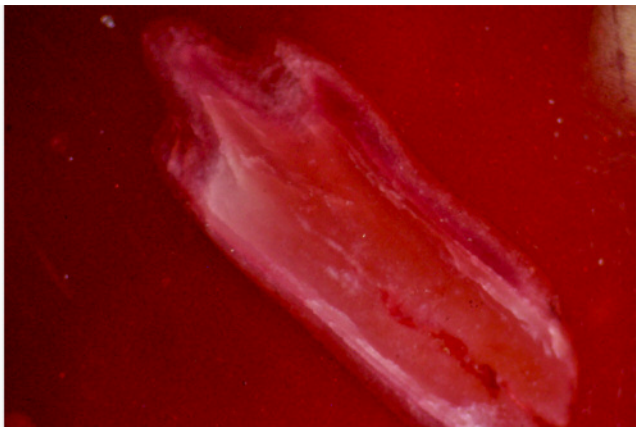

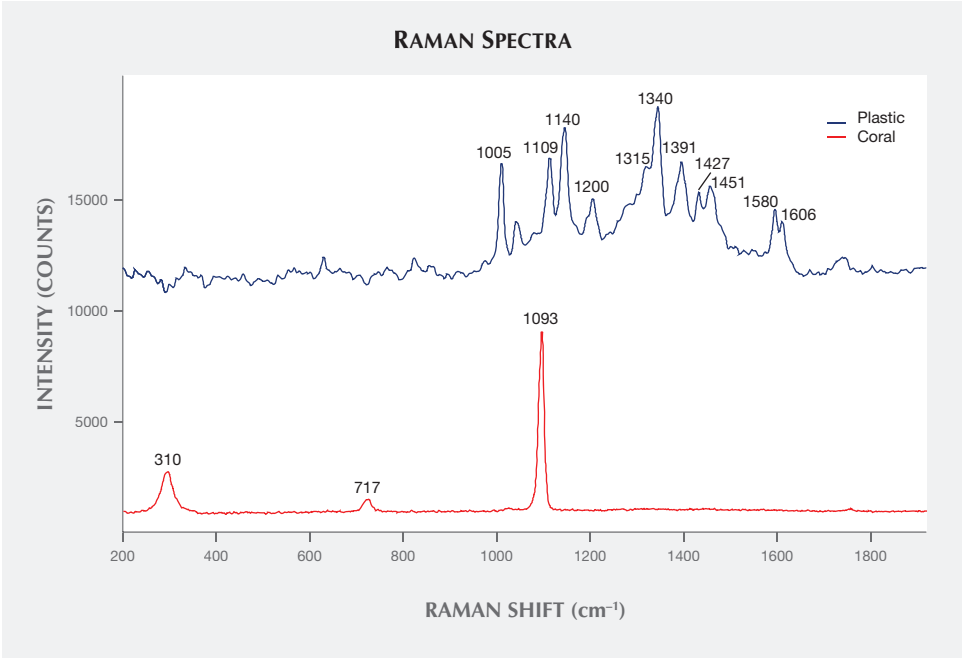

Figure 20. Raman spectra using 785 nm laser confirm that the major component of the bead is plastic (blue trace), while the grains are a carbonate such as calcite (red trace). The lack of carotenoid-related peaks suggests the use of white coral fragments.

approximately 1.53 and hydrostatic SG of 1.97 were obtained. Under UV light, the bead fluoresced orange, with a stronger reaction to SW than LW; a desk-model spectroscope revealed a broad absorption band from the violet to yellow-orange region. Raman spectroscopy (figure 20) confirmed the major component of the bead as plastic, while the grains were identified as carbonate. We did not detect any carotenoid-related peaks, which have been suggested as the cause of color in pink-to red-coral (C.P. Smith et al., "Pink-to-red coral: A guide to determining origin of color," Spring 2007 *G&G*, pp. 4–15). On the basis of Raman spectra and concentric radiating structure, the sharp fragments were identified as white coral.

Coral-plastic composites have been reported previously (e.g., Fall 2008 Lab Notes, p. 253). Further, orange-red plastics have also been known as coral imitations for decades. This specimen turned out to be notable because of the use of coral fragments as inclusions; however, we could not clearly understand its purpose.

Gagan Choudhary (gagan@gjepcindia.com)
Gem Testing Laboratory, Jaipur, India

A jadeite bangle simulant: Hydrogrossular garnet. Jadeite, a material significant within Chinese culture, is often submitted to the Lai Tai-An Gem Laboratory for identification.

Historically, the name "jade" has been applied to either nephrite or jadeite. Nephrite has been used for adornment and ornamentation for thousands of years in China, and nephrite objects from many dynasties are found in muse-

Figure 21. The photo on the left shows a jadeite jade bangle. The photo on the right shows two hydrogrossular garnet bangles that were claimed to be jadeite. Photos by Lai Tai-An Gem Lab.

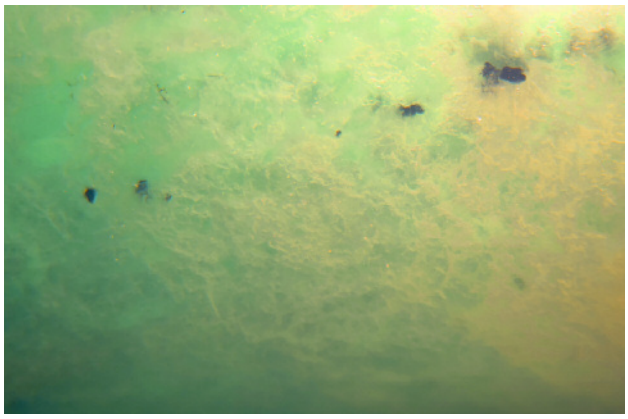

Figure 22. These hydrogrossular garnet bangles exhibit the black pepper-like inclusions that are sometimes found in this material. Photo by Lai Tai-An Gem Lab, field of view 8.20 mm.

ums, auctions, and antique shops around the world. While newer to the Chinese market, jadeite jade is becoming increasingly important. Jadeite bangles (figure 21, left) the require more rough than cabochons or fashioned stones, resulting in a larger amount of waste. Consequently, the value placed on good-quality pieces is higher, and jadeite bangles with fine textures and brilliant colors continue to set new records in auction houses.

Figure 23. FTIR spectra reveal the difference between jadeite jade (red line, peaks at 1175, 1075, 1051, 957, 855, 745, 666, 589, 534, 476, and 435 cm^{-1}) and hydrogrossular garnet (blue line, peaks at 954, 866, 843, 616, 560, 488, and 458 cm^{-1}).

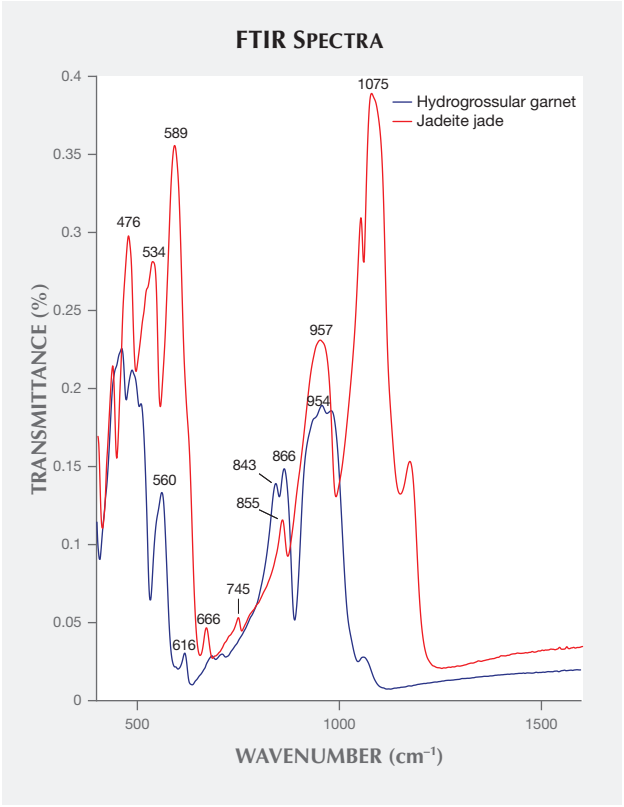

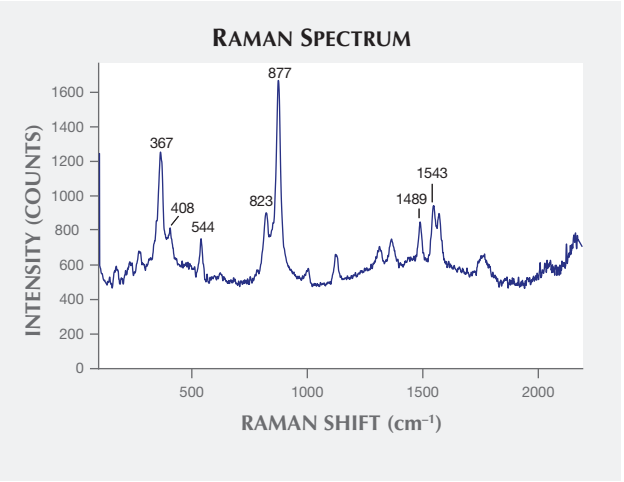

Figure 24. Raman analysis of one of the client's bangles, using a near-infrared wavelength of 785 nm, confirms its hydrogrossular garnet identity.

We recently received two similar-looking bangles (figure 21, right) for identification. The client claimed the pieces were jadeite, but we determined them to be hydrogrossular garnet. This jadeite simulant is rarely seen in bangle form; it is more likely encountered as carvings or cabochons. In this particular case, the similarity to jadeite was extremely convincing.

The two translucent, light to strongly saturated green and white hydrogrossular garnet bangles weighed 339.55 ct and 400.03 ct, and measured 75 × 11 mm and 77 × 12 mm, respectively. Both exhibited a spot RI of 1.72, SG of 3.42/3.45, inert reaction to both SW and LWUV, and a light pink reaction through the Chelsea color filter. The absorption spectrum showed a cutoff below 460 nm, and the material exhibited black pepper-like inclusions (figure 22); these characteristics suggest that the color of the garnet is natural.

The identification was confirmed by FTIR and Raman analysis. Peaks at 954, 866, 843, 616, 560, 488, and 458 cm^{-1} in the infrared spectra (figure 23), and peaks at 367, 408, 544, 823, 877, 1489, and 1543 cm^{-1} (figure 24) in the Raman spectrum are indicative of hydrogrossular garnet. The similarity to jadeite could lead to a costly error, so those in the trade must be aware of such imitations.

Larry Tai-An Lai (service@laitaian.com.tw)
Lai Tai-An Gem Laboratory, Taipei

TREATMENTS

Impregnated and dyed turquoise. Turquoise has a cryptocrystalline structure, which gives rise to the gem's porosity. Its vulnerability to body oils, ordinary solvents, and dirt can induce variation of color. This porous gemstone's ap-

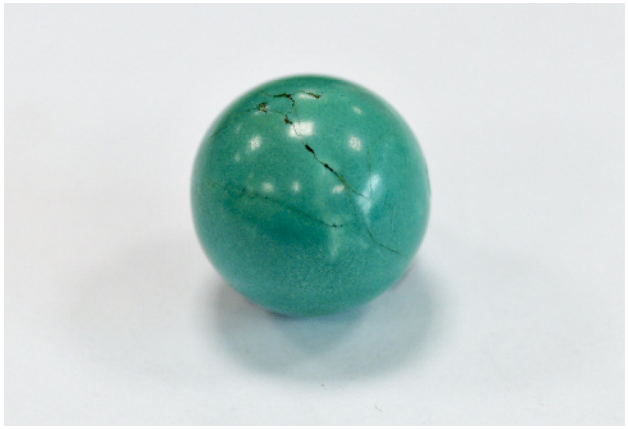

Figure 25. Spectroscopic analysis of this 15.21 gram turquoise reveals that the material has been both impregnated and dyed. Photo by Wen Han.

Figure 26. Some lines, along with the cavity, fluoresce white when exposed to long-wave UV radiation, indicating the presence of filling material. Photo by Wen Han.

pearance and durability can be enhanced by various treatment techniques, such as dyeing, impregnation (with polymer, wax, or plastic), and the proprietary Zachery process (E. Fritsch et al., "The identification of Zachery-treated turquoise," Spring 1999 *G&G*, pp. 4–16).

Turquoise, often featured in vintage jewelry pieces, is becoming increasingly popular in the Chinese market. Recently, the NGTC Beijing lab received for identification a 15.21 gram turquoise sphere with green color (figure 25). The specimen measured approximately 3.5 cm in diameter; its spot RI value was 1.59 and its hydrostatic SG value was 2.58. The test sample was inert, except for several lines and a cavity with moderate white fluorescence under both LW and SWUV radiation (figure 26), suggesting impregnation. Magnification showed some filling material were also present in the cavities. Additionally, green color concentration was observed in the material's cavities and cracks.

Infrared reflectance spectroscopy revealed complicated peaks containing turquoise and impregnated materials. The bands at 1118 and 1050 cm^{-1} were assigned to the asymmetric stretching vibrations of phosphate units, while the 835 cm^{-1} was caused by the bending vibration of OH units. Other features from approximately 647 to 482 cm^{-1} were due to the phosphate bending modes of turquoise. The 2918 and 2850 cm^{-1} peaks were attributed to wax; additionally, a series of small peaks from 1800 to 1350 cm^{-1} indicated the

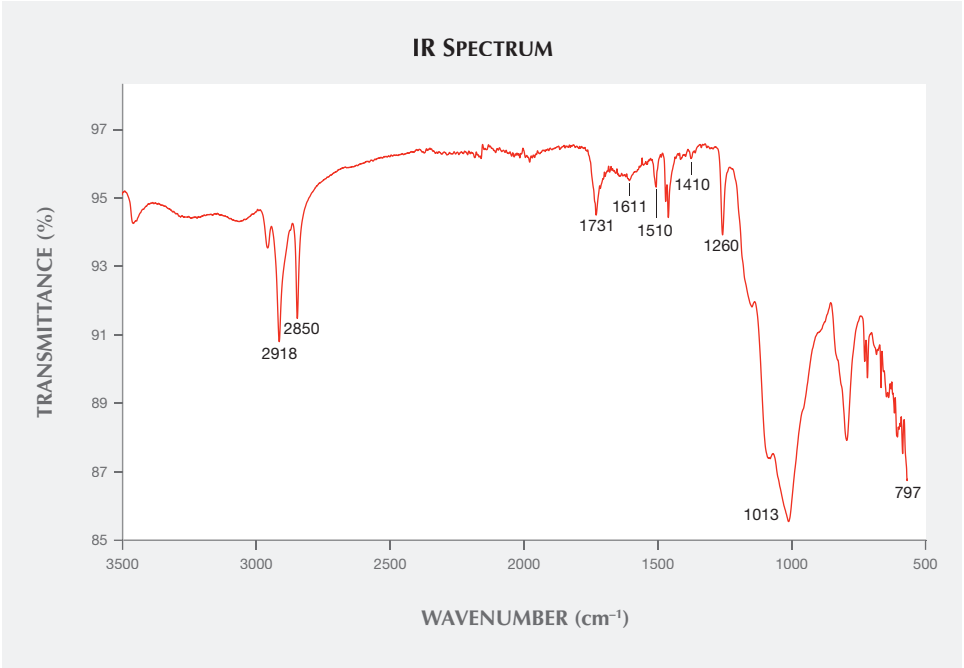

Figure 27. The infrared transmittance spectrum of small amounts of powder scraped from the sample shows that the turquoise was impregnated with three components: epoxy resin, acrylic polymer, and silicone.

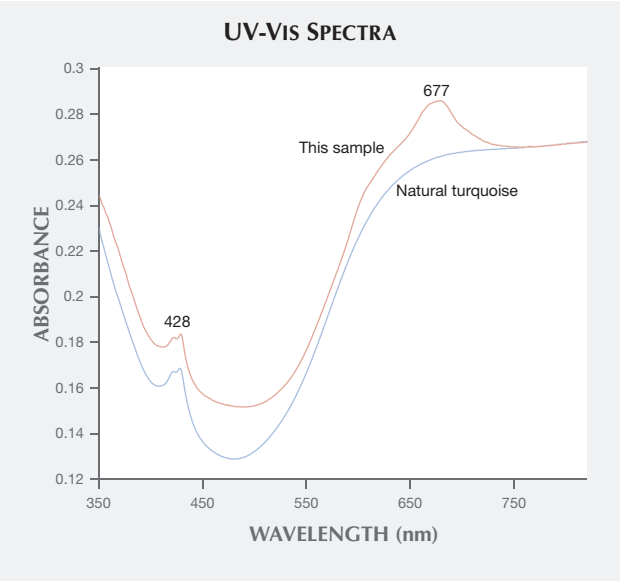

Figure 28. When compared with the spectrum of a known natural turquoise sample, the 677 nm band of the UV-VIS spectrum indicates that the sample in this study was dyed.

presence of organic matter. To identify this organic material, we scraped off some powder from the edge of one of the cavities with a blade. The resulting infrared transmittance spectrum indicated the presence of three kinds of polymer (figure 27). The 1731 and 1013 cm^{-1} peaks were attributed to acrylic polymer, and the 1611 and 1510 cm^{-1} peaks were due to epoxy resin; both are commonly applied to various gem materials for impregnation. Peaks at 1410, 1260, and 797 cm^{-1} were characteristic absorption features of silicone. Silicones are polymers consisting of repeating units of siloxane (a functional group composed of two silicon atoms and one oxygen atom, often combined with carbon and hydrogen). The 1410 and 1260 cm^{-1} peaks were caused by asymmetric and symmetric deformation vibrations of Si-CH_3, respectively, and the 797 cm^{-1} was assigned to the Si-C stretching vibrations of the silicones.

EDXRF chemical analysis detected mainly P, Al, Cu, Fe, and Si. The first four are consistent with the chemical composition of turquoise, while Si was suspected to be a byproduct of silicone impregnation. The UV-Vis spectrum showed two absorption bands: a band centered at about 428 nm caused by Fe^{3+} d-d electronic transition, and a sharp band centered at approximately 677 nm (figure 28). Natural-color turquoise does not show the 677 nm band; many Chinese labs consider this feature characteristic of dyed material.

Turquoise is usually impregnated with acrylic polymer or epoxy resin for stabilization in addition to the dyeing process to change its color. This is the first time we have encountered turquoise that was dyed and impregnated with three components. Our investigation reinforces the need to identify any and all treatments.

Wen Han (winnerzx@126.com), Taijin Lu, Huiru Dai, and Jun Su
National Gems & Jewelry Technology Administrative Center (NGTC)
Beijing

Hui Dai
Institute of Geological Experiment of Anhui Province
Hefei, China

ERRATA

1. In the Summer 2015 article by E. Sorokina et al., "Rubies and Sapphires from Snezhnoe, Tajikistan," coauthor Dr. Andrey K. Litvinenko was incorrectly listed as director of GIA Moscow.

2. In the Summer 2015 GNI entry "Crimson Prince ruby from Namya" (pp. 214–215), the location of Namya was incorrectly shown on the map. The location has been corrected in the online versions (HTML and PDF) of the Summer 2015 issue.

IN MEMORIAM
TINO HAMMID (1952 2015)

Gems & Gemology mourns the loss of acclaimed gem and jewelry photographer Tino Hammid, who died July 11 at the age of 63 after a two-year battle with cancer. Mr. Hammid is widely remembered throughout the industry for his kindness and his passion for the craft.

The son of Academy Award–winning filmmaker Alexander Hammid, the New York native established his career in Los Angeles. From 1980 to 1982, he served as a staff photographer at GIA's Santa Monica campus. Upon leaving GIA, he became a successful freelance photographer, capturing some of the world's most remarkable gems.

In 1983, he began photographing gemstones for David Federman's popular Gem Profile column in each monthly issue of *Modern Jeweler*. Their 25-year collaboration yielded two Jesse H. Neal awards for business journalism and a pair of Gem Profile hardcover volumes: *The First 60* (1988) and *The Second 60* (1992). Mr. Hammid's work appeared in countless other books, and starting in 1987 he photographed more than 100 Christie's jewelry auction catalogs.

G&G has been privileged to showcase Mr. Hammid's talents for over 30 years. Longtime readers of the journal will recognize his distinctive backgrounds and use of light and shadow. Through his style and technique, he exerted a lasting influence on gem photography. Tino Hammid is survived by his wife, Petra, and three children. We extend our deepest condolences to his family and friends.